Solar radiation and thermal performance of solar collectors for Denmark

Janne Dragsted
Simon Furbo

Report

Department of Civil Engineering
2012

DTU Civil Engineering Report R-275 (UK)
October 2012

DTU Civil Engineering
Department of Civil Engineering

DTU BYG

Department of Civil Engineering

2012

Byg Rapport R-275

ISBN 9788778773593

Content

Introduction

This report describes the part of the EUDP project “EUDP 11-I, Solar Resource Assessment in Denmark”, which is carried out at Department of Civil Engineering, Technical University of Denmark. The other part of the project is carried out at DMI and described in [4].

1. Measured solar radiation from 2006 to 2010

The climate station at DTU has since 1989 measured the solar radiation. The measurements consist of global, beam and diffuse radiation and are obtained with a time step of 2 minutes. Based on the measurements from 2006 to 2010 the most commonly used mathematical models for determining the diffuse radiation will be evaluated on an hour basis.

- Global radiation is measured with a CM11 pyranometer by Kipp and Zonen. The value is an instant value of the global radiation every two minutes.
- Diffuse radiation is measured either with a tracker that block out beam radiation or with a shadow band, both measurements are obtained with a CM 11 pyranometer by Kipp and Zonen. The values are instant values every two minutes.

The measurements of the diffuse radiation obtained with the tracker have a higher accuracy than the measurements with the shadow band, why preferably the measurements from the tracker are used in the study. In the cases where the tracker has not had the right position and has not shielded the beam radiation, the measurement with the shadow band is used. The correction for the shadow band has been carried out according to the description in [1].

The data has been sorted in order to remove faulty measurements.

During the 5 years that the measurements have been collected there has been times when the data logger was out of order. For missing data in a time period of less than one hour, the data has been regenerated by interpolation. For missing data for more than an hour the data is simply left missing.

In Table 1 the yearly values of the global radiation, diffuse radiation on horizontal and beam,n radiation are shown. Also shown is the percentage of available measurements. It can be seen that 2009 has the highest values in terms of the global and beam,n radiation. The values from 2008 and 2010 are low, but this can be explained by the high degree of missing data. Due to the lacking data, the yearly solar radiation in table 1 cannot be compared with other datasets with full years of data.

Table 1 The yearly solar radiation from 2006 to 2010.

Yearly solar radiaton	Global radiation	Diffuse radiation on horizontal	Beam,n radiation	Available measurements
	[kWh/m²]	[kWh/m²]	[kWh/m²]	[%]
2006	984	471	1014	98.2
2007	967	484	961	98.4
2008	918	424	957	91.8
2009	1034	482	1068	98.0
2010	905	481	847	96.6

On Figure 1 to Figure 5 the hour values of the global, diffuse and beam,n radiation from 2006 to 2010 are shown. The hour values are generated based on the 2 minute measurements.

The missing data seen on the figures are when the data logger is out of order for more than an hour and there are no data available.

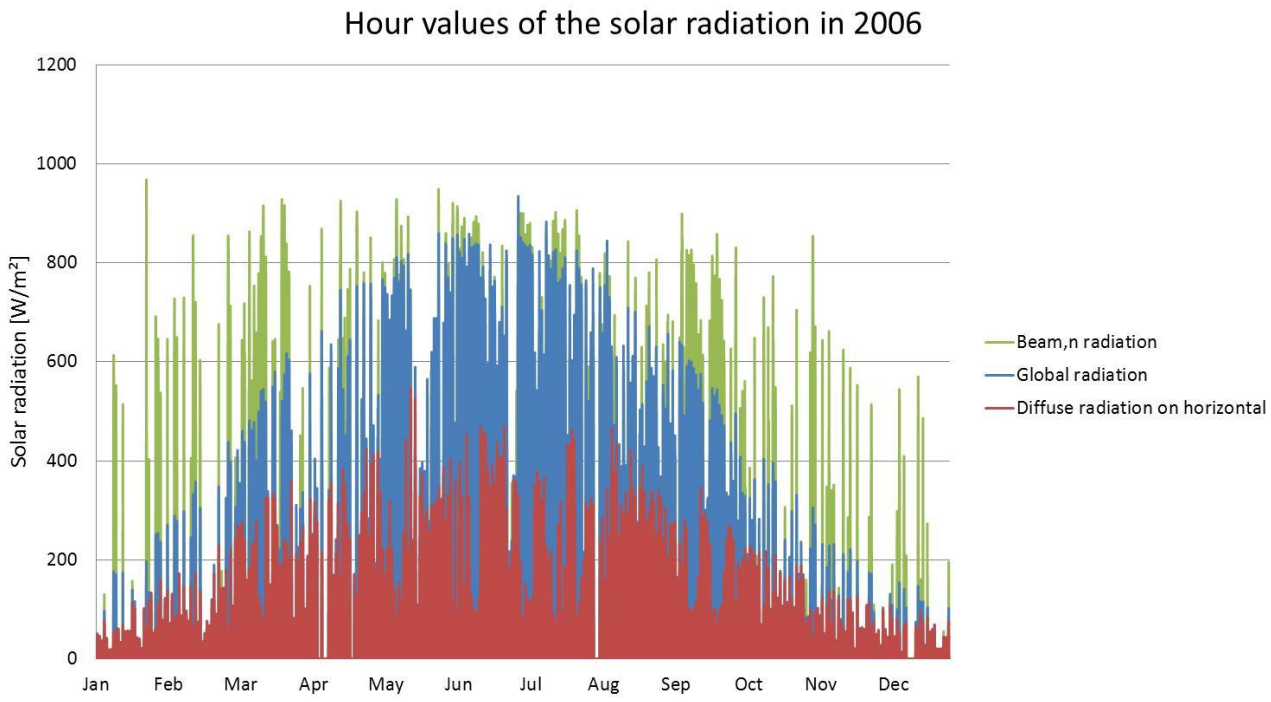

Figure 1 The hour values of the solar radiation in 2006 based on the two minute measurements.

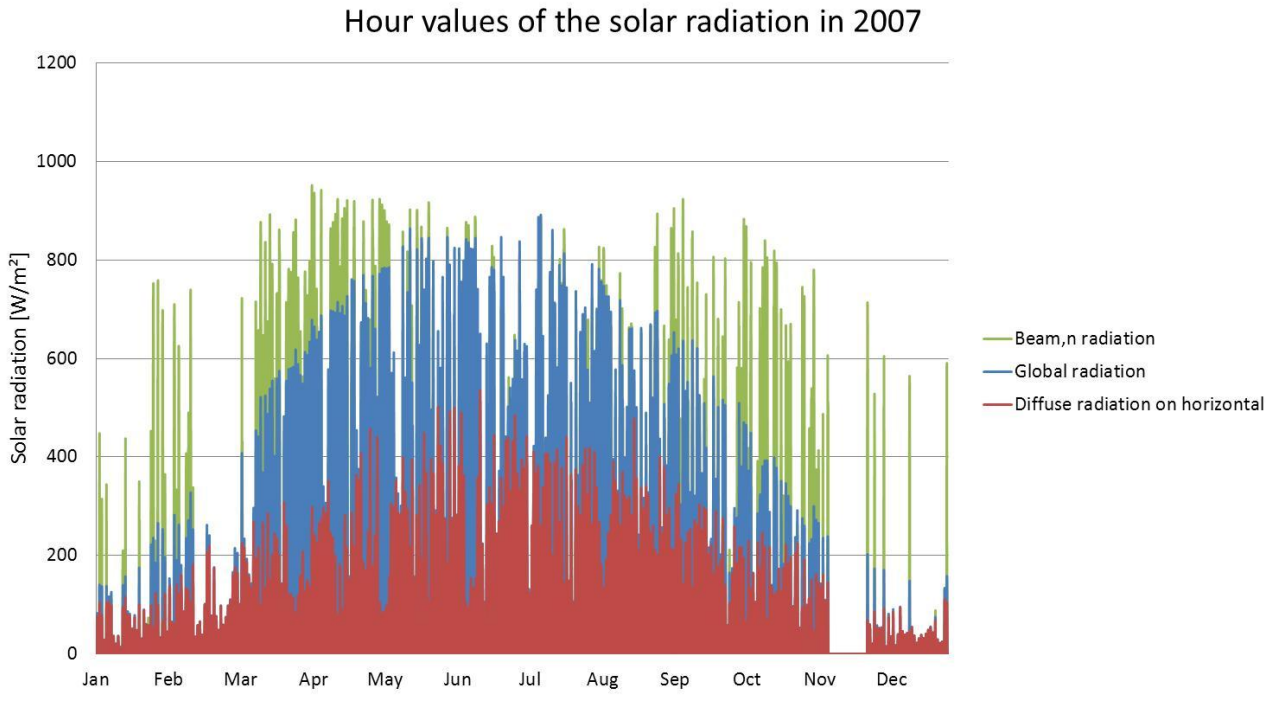

Figure 2 The hour values of the solar radiation in 2007 based on the two minute measurements.

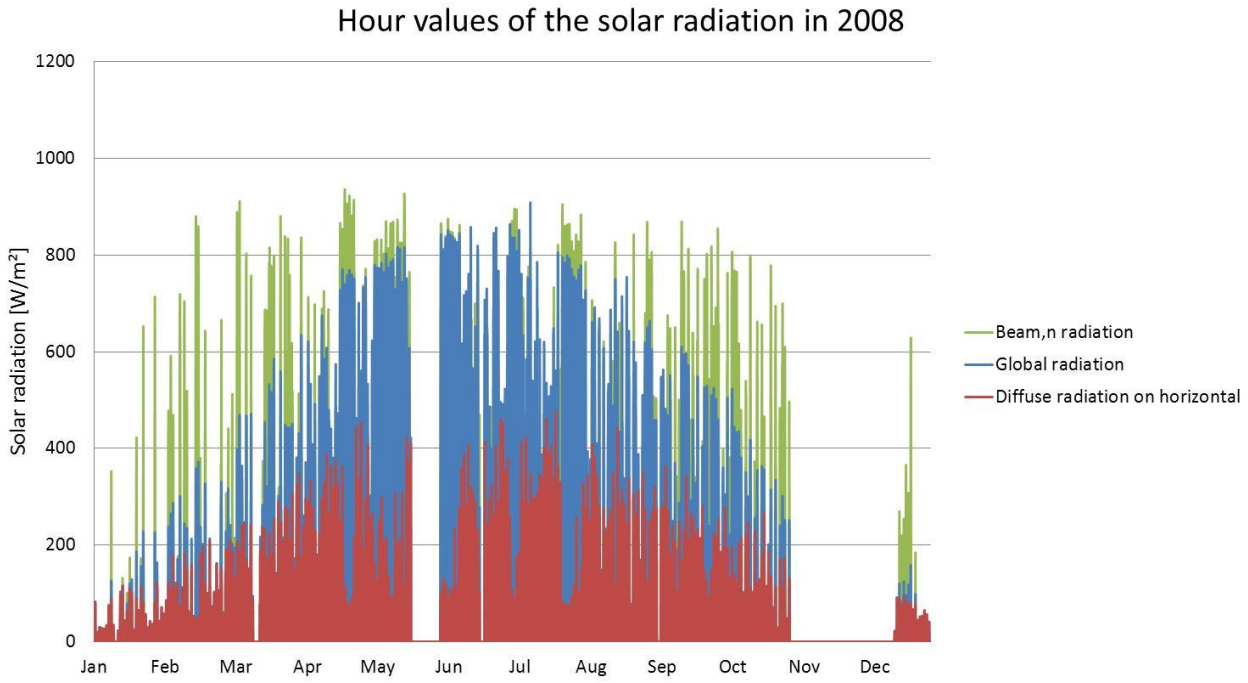

Figure 3 The hour values of the solar radiation in 2008 based on the two minute measurements.

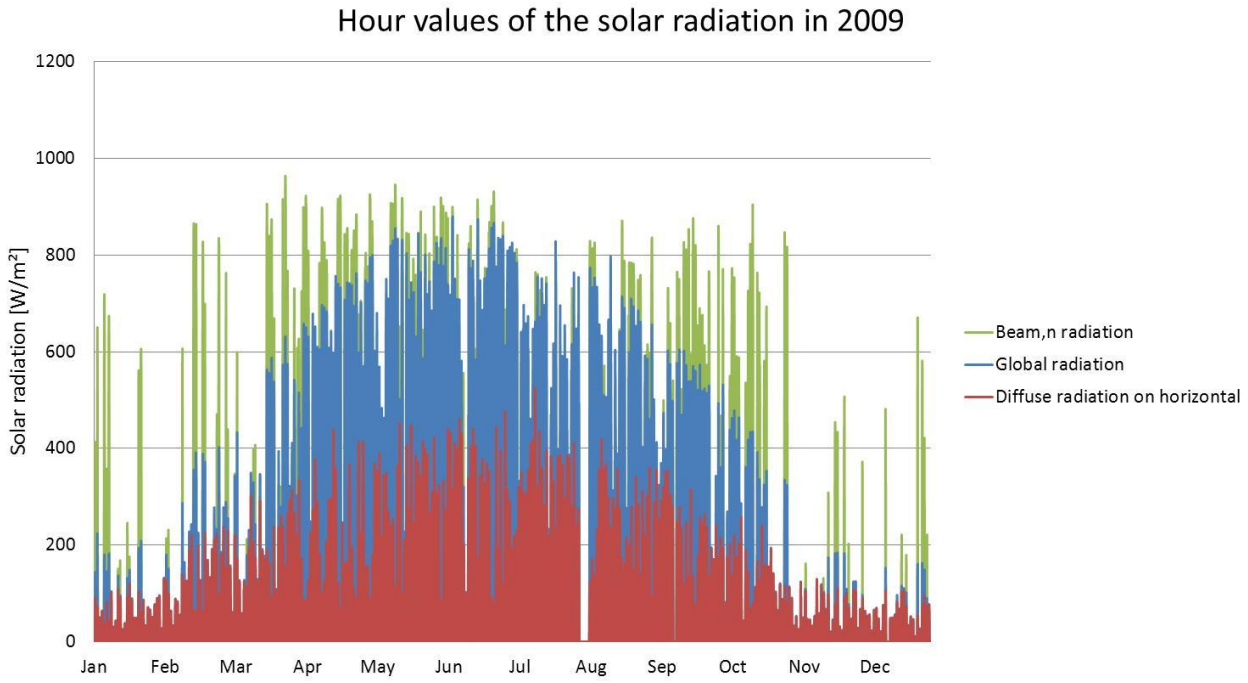

Figure 4 The hour values of the solar radiation in 2009 based on the two minute measurements.

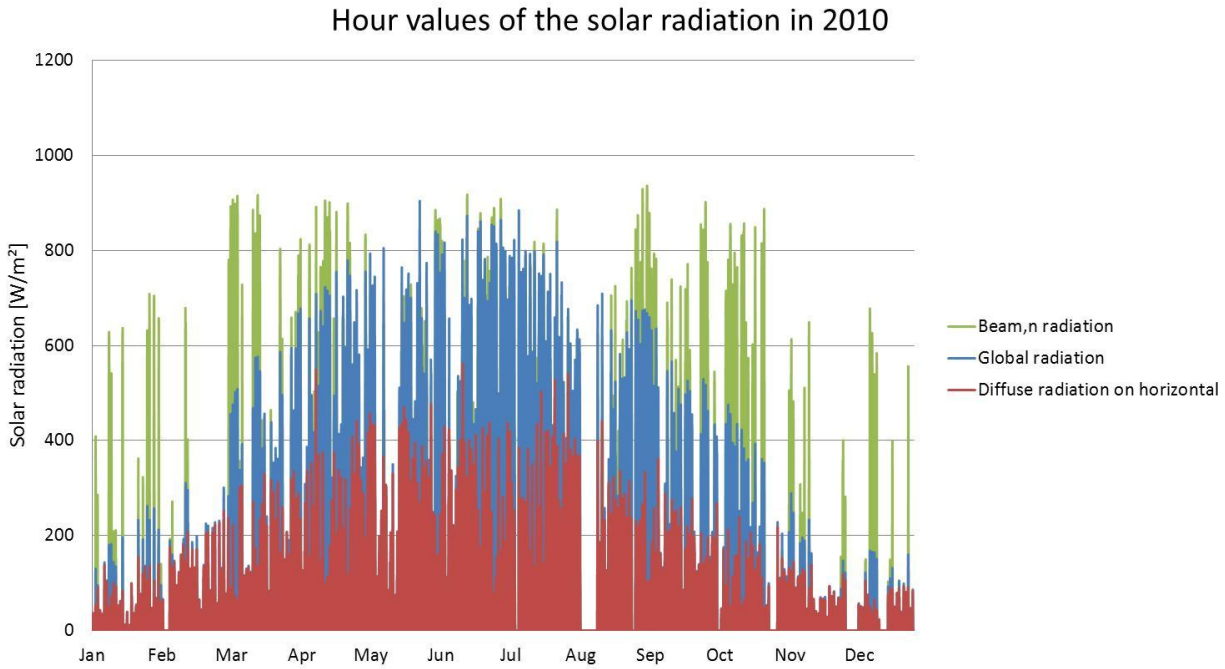

Figure 5 The hour values of the solar radiation in 2010 based on the two minute measurements.

2. Diffuse correlation

The diffuse correlation describes the relationship between the diffuse radiation and the global radiation on a horizontal surface. On Figure 6 the correlation between the hour values of diffuse radiation on a horizontal surface and the hour values of the global radiation is shown as a function of the clearness index. The clearness index is the ratio between the hour values of the global radiation and the calculated extraterrestrial radiation. Each dot on the figure corresponds to a 1 hour value.

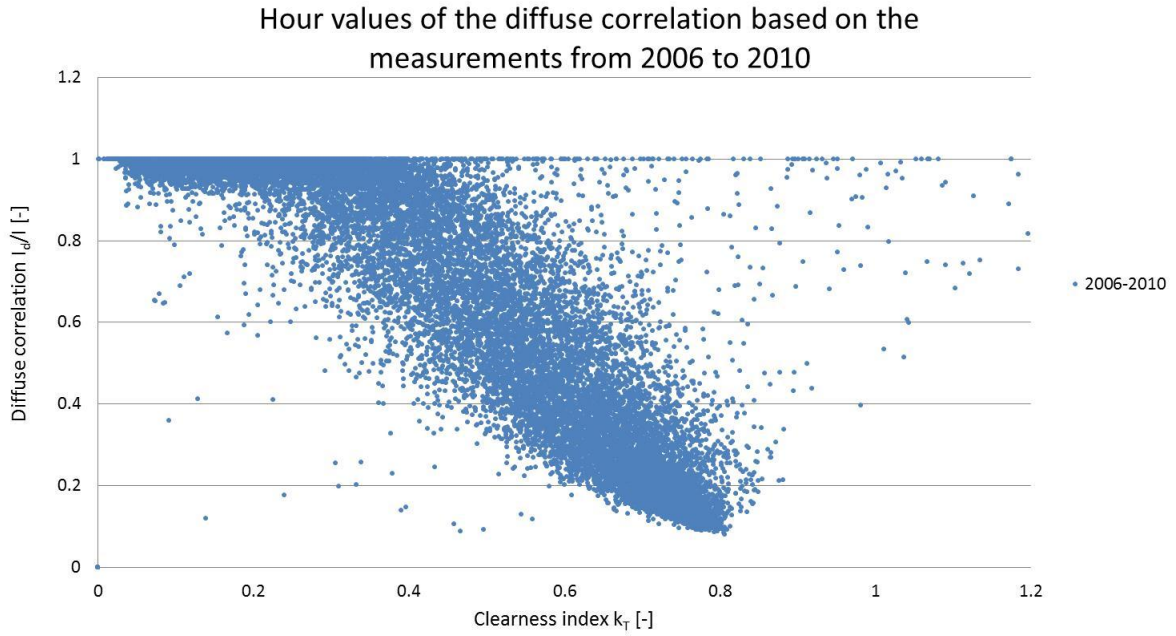

Figure 6 The calculated hourly diffuse correlation based on the measurements from 2006 to 2010.

For a small clearness index the diffuse correlation is close to 1, and therefore the global and diffuse radiation are the same, which is seen on overcast days. The values on a sunny day are seen at a clearness index around 0.7, corresponding to the diffuse radiation being 10 % of the global radiation. For higher values of the clearness index the global radiation receives additional radiation in the form of inter reflected radiation from the sky and drifting clouds.

The correlation between the diffuse and global radiation on horizontal for all 5 years is weighed against the global radiation. The weighing is carried out for small intervals of the clearness index by:

$$\frac{\sum\left(\frac{I_d}{I}.I\right)}{\sum I}$$

The weighted values of the diffuse correlation for all 5 years are shown on Figure 7, along with the average of the weighted values.

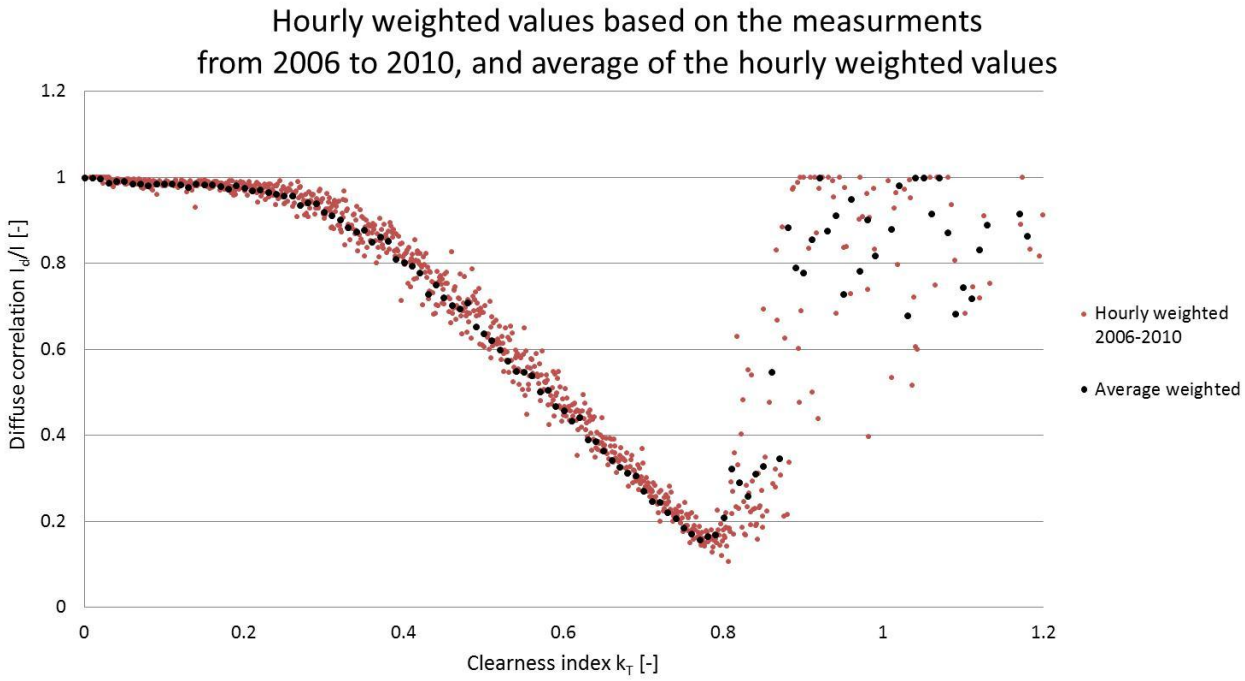

Figure 7 The weighed values of the diffuse correlation for all 5 years.

3. Commonly used mathematical models

The three most commonly used diffuse correlations are from 'Erbs et al', 'Orgill and Hollands' and 'Skarveit and Olseth' [2], [3]. In the following the correlations are presented along with a diffuse correlation determined based on the measurements from DTU, 'DTU equation'.

3.1. Erbs et al.

'Erbs et al.' is defined by:

$k_T \leq 0.22$	$I_d/I = 1.0 - 0.09\ k_T$
$0.22 < k_T \leq 0.80$	$I_d/I = 12.336\ k_T^4 - 16.638\ k_T^3 + 4.388\ k_T^2 - 0.1604\ k_T + 0.9511$
$k_T > 0.80$	$I_d/I = 0.165$

3.2. Orgill and Hollands

'Orgill and Hollands' is defined by:

$k_T < 0.35$	$I_d/I = 1.0 - 0.249\ k_T$
$0.35 \leq k_T \leq 0.75$	$I_d/I = 1.557 - 1.84\ k_T$
$k_T > 0.75$	$I_d/I = 0.177$

On Figure 8 the average hourly weighted values based on the measurement are shown along with 'Erbs et al.' and 'Orgill and Hollansd'. It is here seen that for values of the clearness index less than 0.75 there is a good agreement between the measurements and the calculated values. For values of the clearness index higher than 0.75 the prediction that the diffuse correlation assumes a constant value is not in agreement with the measurements.

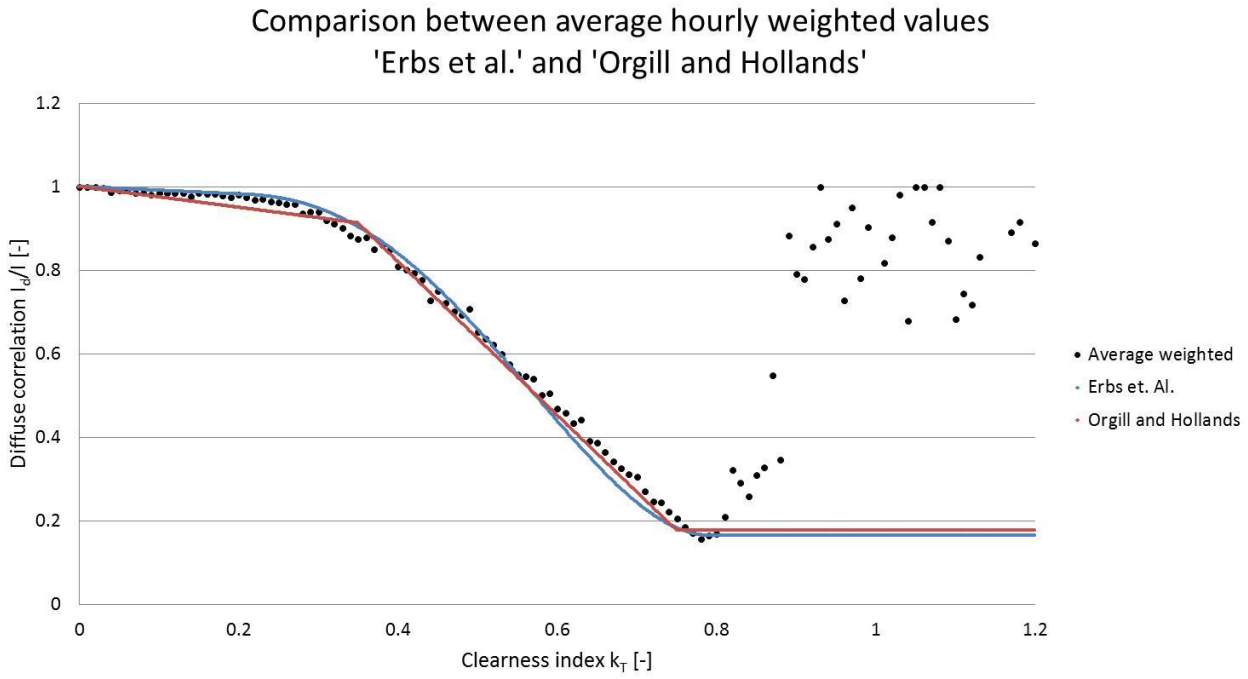

Figure 8 The average hourly weighted values compared with 'Erbs et al.' and 'Orgill and Hollands'.

3.3. DTU equation

The 'DTU equation' is based on the average values of the hourly weighted values, and is divided into 4 intervals of the clearness index.

$k_T = 0.00 – 0.29$ $\quad I_d/I = -6.0921\ k_T^3 + 1.9982\ k_T^2 – 0.2787\ k_T + 1$

$k_T = 0.29 – 0.72$ $\quad I_d/I = 3.99\ k_T^3 – 7.1469\ k_T^2 + 2.3996\ k_T + 0.746$

$k_T = 0.72 – 0.80$ $\quad I_d/I = 288.63\ k_T^4 – 625.26\ k_T^3 + 448.06\ k_T^2 –105.84\ k_T$

$k_T = 0.80 – 1.20$ $\quad I_d/I = 65.89\ k_T^4 – 210.69\ k_T^3 + 222.91\ k_T^2 – 77.203\ k_T$

On Figure 9 the average values of the hourly weighted values are shown along with the 'DTU equation'. The figure shows a good correlation between the measured and the calculated values. For values of the clearness index higher than 0.75 the agreement between measured and calculated in reduced.

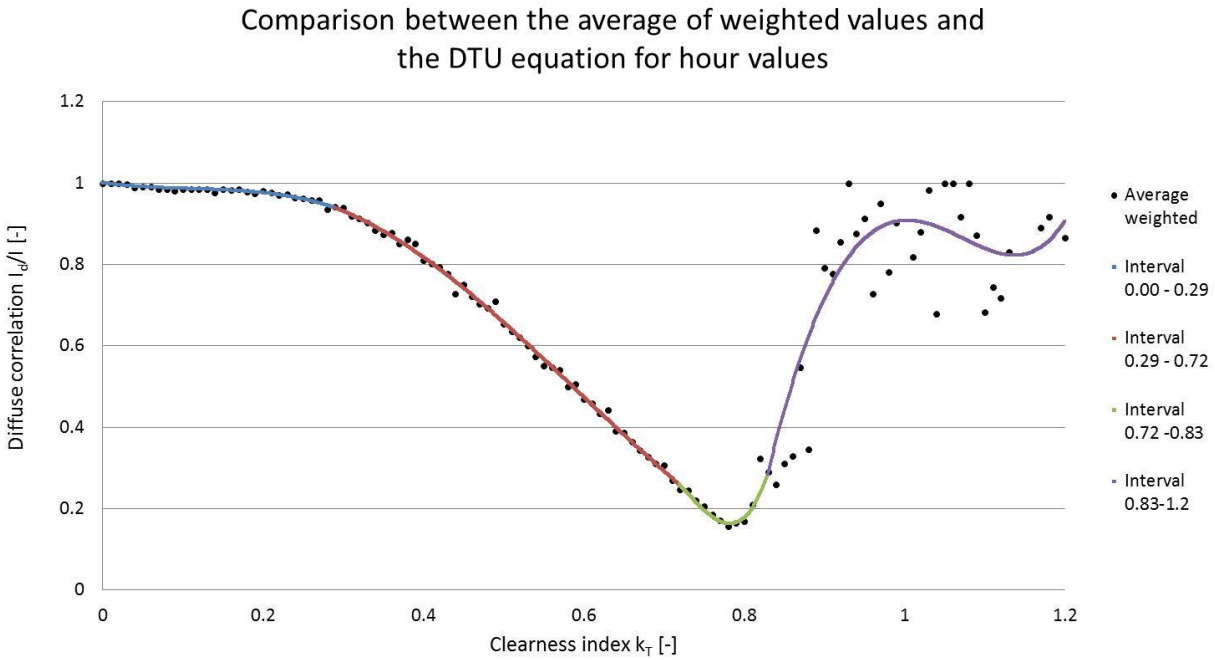

Figure 9 The comparison between the average of the weighed values and the DTU equation for hour values.

3.4. Skartveit and Olseth

In the model by 'Skartveit and Olseth' a variability index is introduced, taking into account the effects of drifting clouds by looking to the values of following and preceding time step.

'Skartveit and Olseth' is defined by:

$$k_T \leq 0.22 \qquad d = 1.0$$

$$0.22 \leq k_T \leq k_2 \qquad d = 1 - (1 - d_1) \cdot \left(0.11\sqrt{K} + 0.15K + 0.74K^2\right)$$

$$k_2 \leq k_T \leq k_{max} \qquad d = d_2 k_2 (1 - k_T)/\left(k_T(1 - k_2)\right)$$

$$k_T \geq k_{max} \qquad d = d_2 k_2 (1 - k_T)/\left(k_T(1 - k_2)\right)$$

Where k_{max} is given as:

$$k_{max} = \left(0.81^{(1/\sin(h))^{0.6}} + d_2 k_2/(1 - k_2)\right)/(1 + d_2 k_2/(1 - k_2))$$

The diffuse correlation is found by:

$$I_d/I = d \cdot \Delta(k, h, \sigma^3)$$

The agreement between the hourly values of the diffuse correlation based on the measurements and the calculations with 'Skartveit and Olseth' are shown on Figure 10.

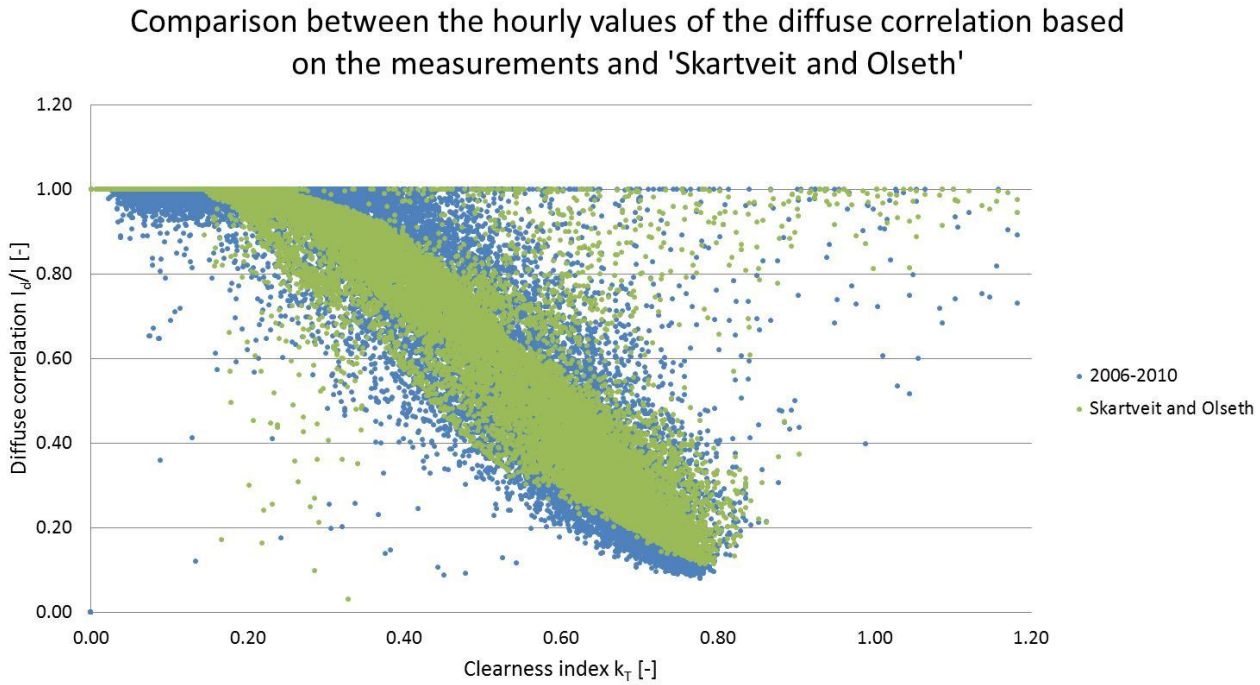

Figure 10 The comparison between the hourly values of the diffuse correlation based on the measurements and 'Skartveit and Olseth'.

On Figure 11 the procedure of the weighing is applied both on the measurements and on the calculated values from 'Skartveit and Olseth'. The results show a good agreement between the measured and calculated values with 'Skarveit and Olseth'.

Figure 11 The comparison between the weighted values based on the measurements and calculated with 'Skartveit and Olseth'

4. Accuracy of the different mathematical models

The deviation between the measurements and the calculated values is evaluated by the Root mean square method. Values for the clearness index higher than 1 are disregarded, since the models of 'Erbs' et al.' and 'Orgill and Hollands' are not intended for these values.

The deviation is determined by:

$$\sqrt{\frac{\sum_{i=1}^{n}\left(\frac{I_d}{I_{measured}}-\frac{I_d}{I_{calculated}}\right)^2}{n}}$$

4.1. Yearly deviation

The overall result for the 5 years is seen in Table 2.

Table 2 The overall result of the Root mean Square method.

Erbs et al.	Orgill and Hollands	DTU equation	Skartveit and Olseth
0.15	0.15	0.12	0.13

In Table 3 the result is shown on a yearly basis.

Table 3 The yearly deviation in percentage between the measured diffuse radiation and the calculated values.

	Erbs et al.	Orgill and Hollands	DTU equation	Skartveit and Olseth
2006	-4	-3	0	-2
2007	-4	-4	0	-2
2008	0	0	3	2
2009	-6	-5	-1	-2
2010	-5	-5	-2	-1

4.2. Monthly deviation

Although the 'DTU equation' returns a lower RMS value on yearly basis, when viewing the results on a monthly basis the model from 'Skartveit and Olseth' returns a slightly better result in the months with a high amount of solar radiation, see Figure 12.

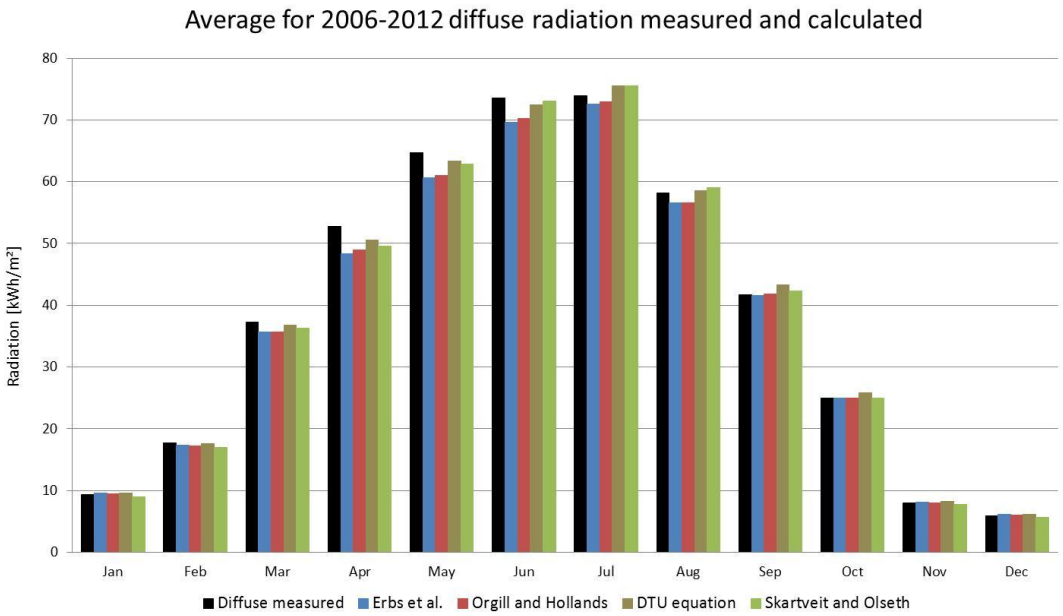

Figure 12 The comparison between average measured and calculated diffuse radiation for 2006 to 2010.

On Figure 13 the average monthly deviation between the measured and the calculated values for the diffuse radiation is show in %, along with the average monthly values of the global radiation.

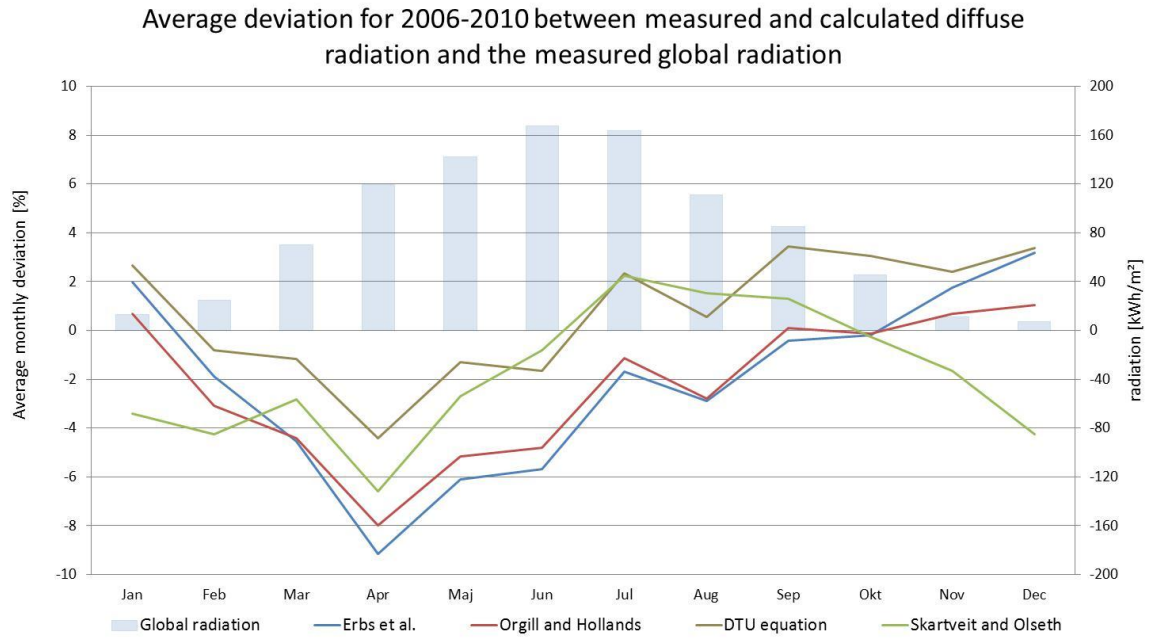

Figure 13 The average monthly deviation for 2006 to 2010 between the measured and calculated diffuse radiation along with the average measured monthly global radiation.

4.3. Daily deviation

In the following a selection of days from 2006 is shown, with the measured global and diffuse radiation along with the calculated values, see Figure 14 to Figure 18. The figures show a spring day with light cloud cover (Figure 14) and with dense cloud cover (Figure 15). Also a spring and summer day with scattered cloud cover (Figure 16 and Figure 18), and a summer day with clear sky (Figure 17).

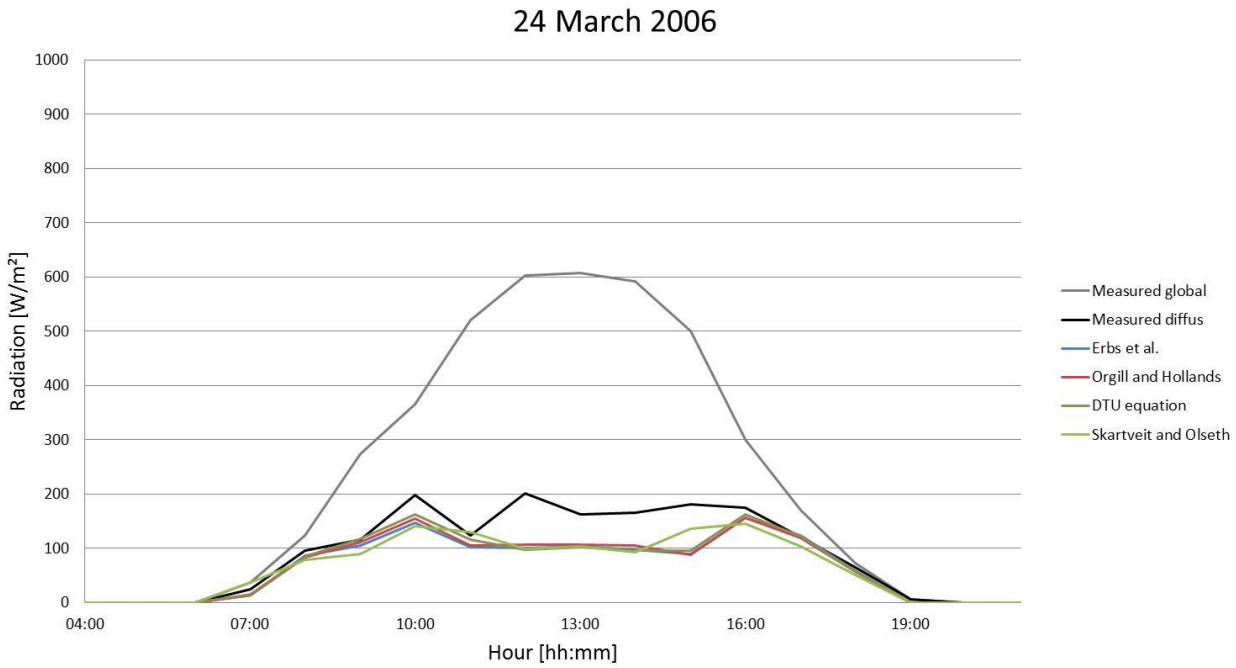

Figure 14 The measured and calculated radiation on March 24th 2006.

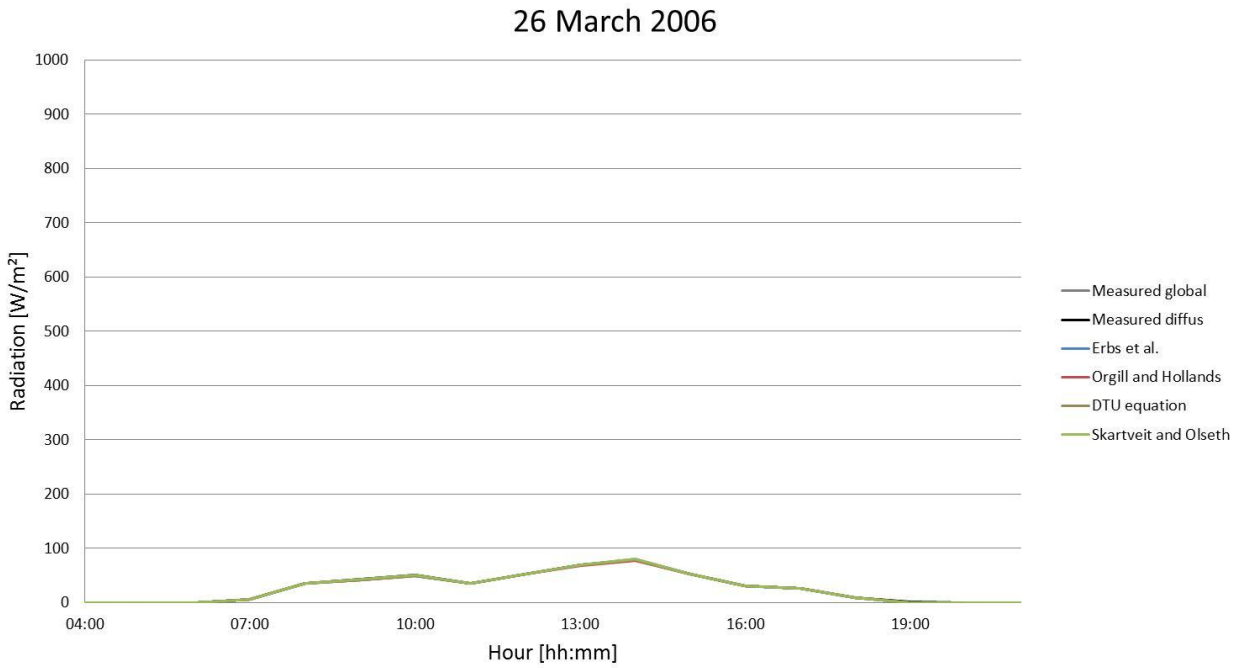

Figure 15 The measured and calculated radiation on March 26th 2006.

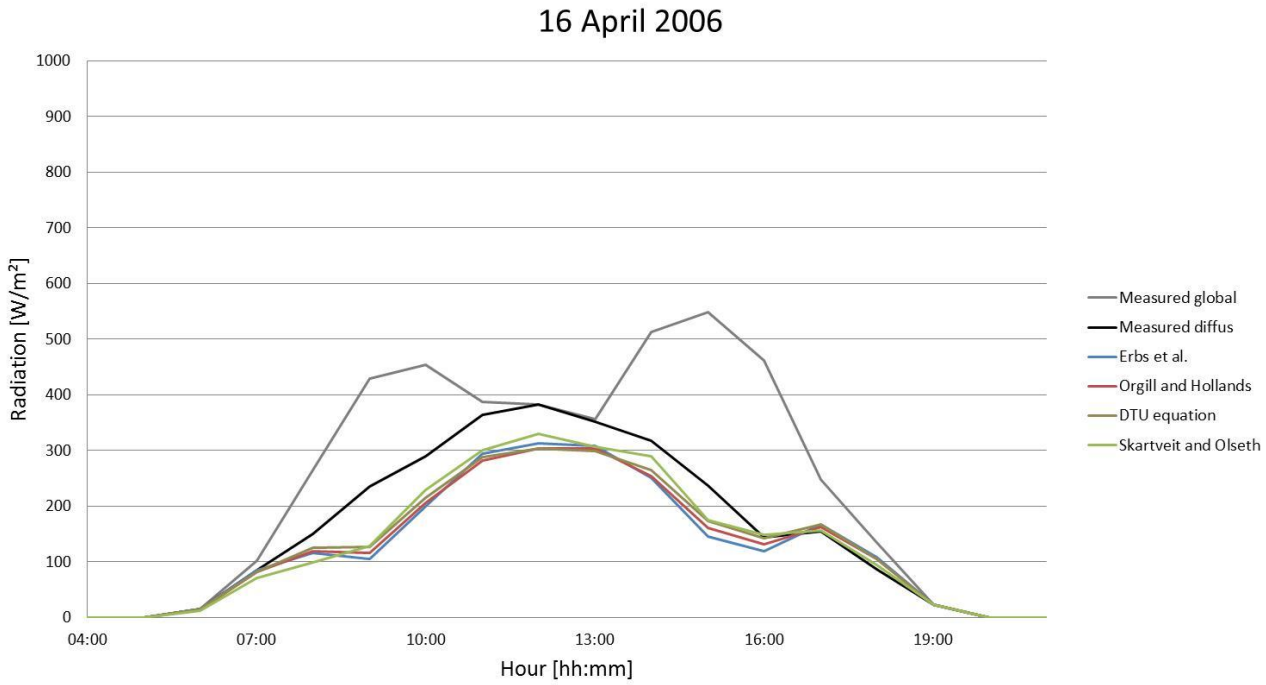

Figure 16 The measured and calculated radiation on April 16th 2006.

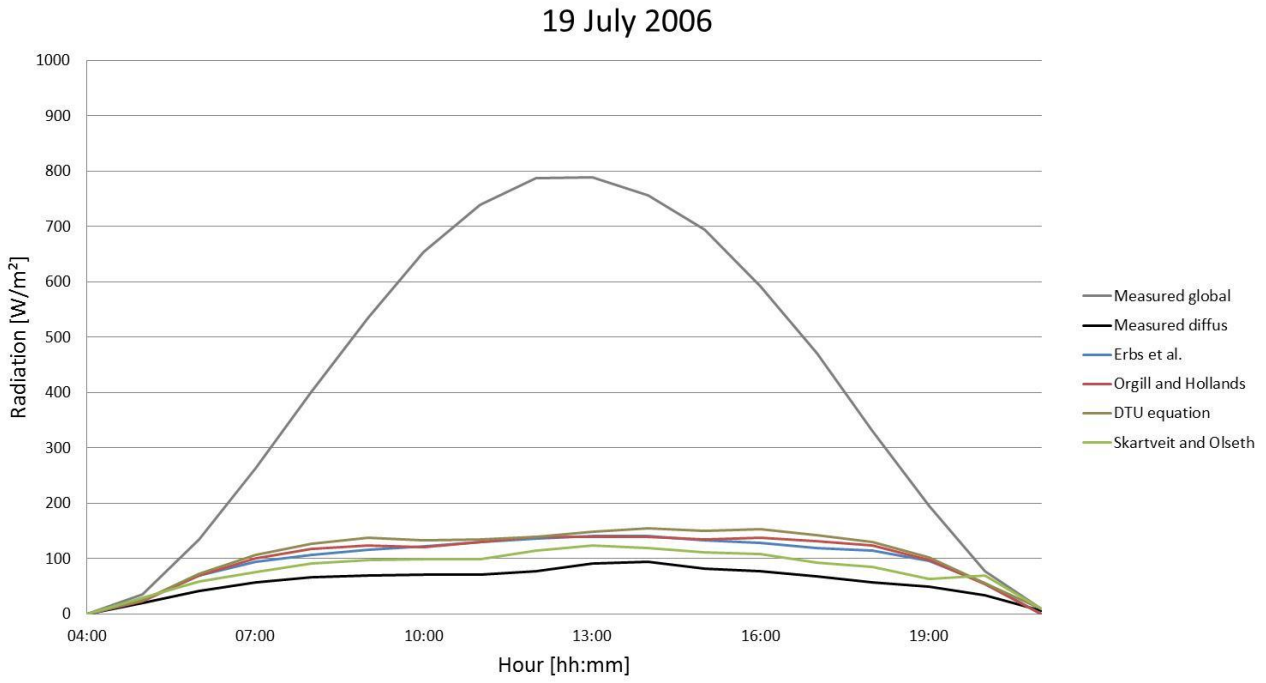

Figure 17 The measured and calculated radiation on July 19th 2006.

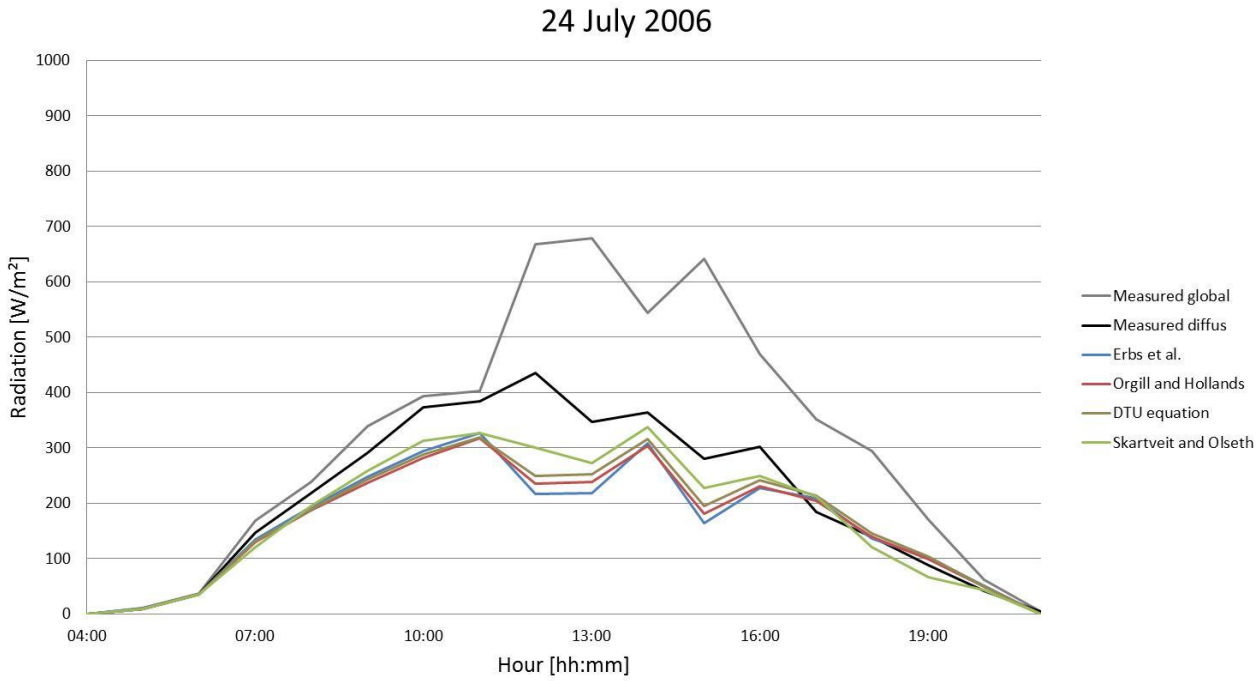

Figure 18 The measured and calculated radiation on July 24th 2006.

The figures shown that the model from 'Skartveit and Olseth' gives the best result on clear sky days and days with drifting clouds. On overcast days all models perform well.

Based on the results it is recommended that the model from 'Skartveit and Olseth' is used when calculation of the diffuse radiation is necessary.

5. Thermal performance of solar collectors for new Design Reference Years

New Design Reference Years for solar energy utilization have been developed for 19 different regions of Denmark [4]. The weather data for the Design Reference Years are based on measurements at DMI's climate stations for the period 2001-2010.

Measured hourly values for four parameters are used in connection with dividing Denmark into the 19 regions: Global radiation, outdoor temperature, wind velocity and air humidity. Denmark is divided into 5 or 6 regions for each parameter resulting in a total of 19 regions. The 19 regions are: Bornholm, central East Zealand, the coast of East Zealand, central West Zealand, the coasts of South and West Zealand & East Funen and the islands from Samsø to Møn, central Lolland-Falster, the middle and eastern part of Funen, central West Funen, the coast of West Funen, the coast of East Jutland, central Jutland, the coast of West Jutland, Salling, central Jutland, the coast of East Djursland and Mols, the coasts of East Jutland and Vendsyssel, central Vendsyssel, Thy & the Skaw & Læsø and Anholt.

The weather data for the new Design Reference Years are hourly values for the four above mentioned parameters and for the diffuse radiation on horizontal determined by the method developed by Skartveit and Olseth as described in chapter 3.4.

Figure 19 shows the 6 regions with different global radiations and Figure 20 shows the 6 regions with different outdoor temperatures.

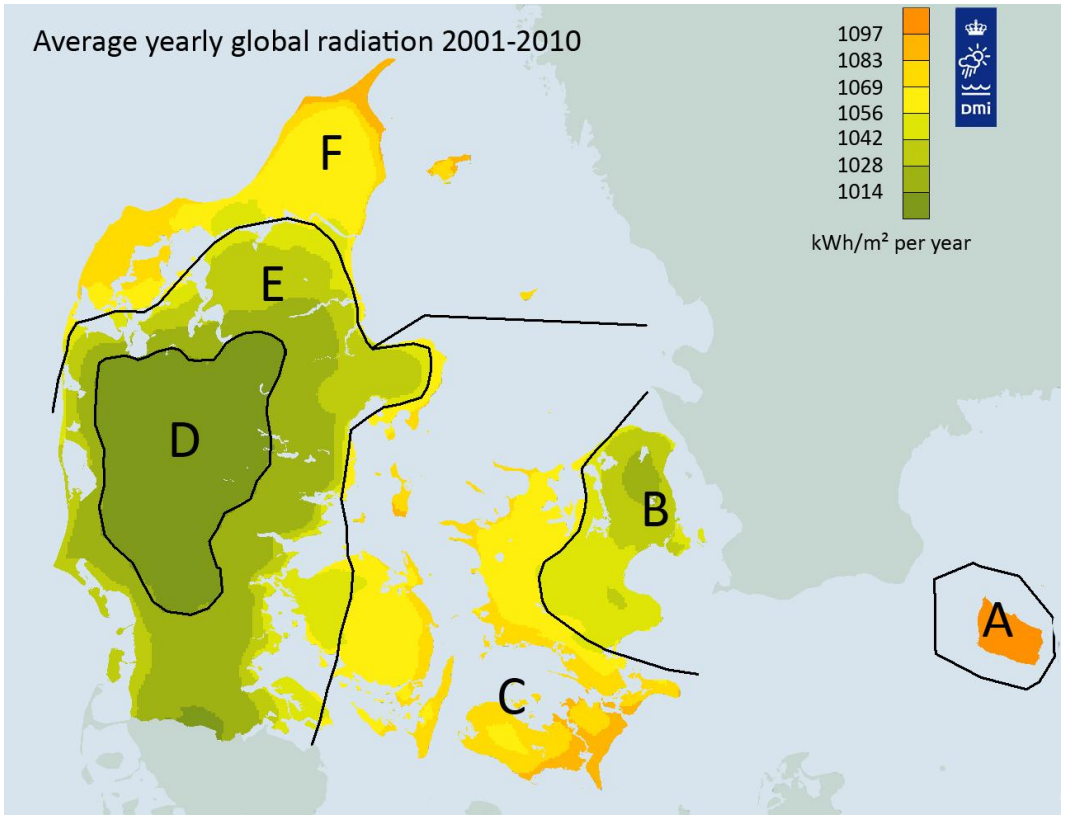

Figure 19 The regions with different global radiations.

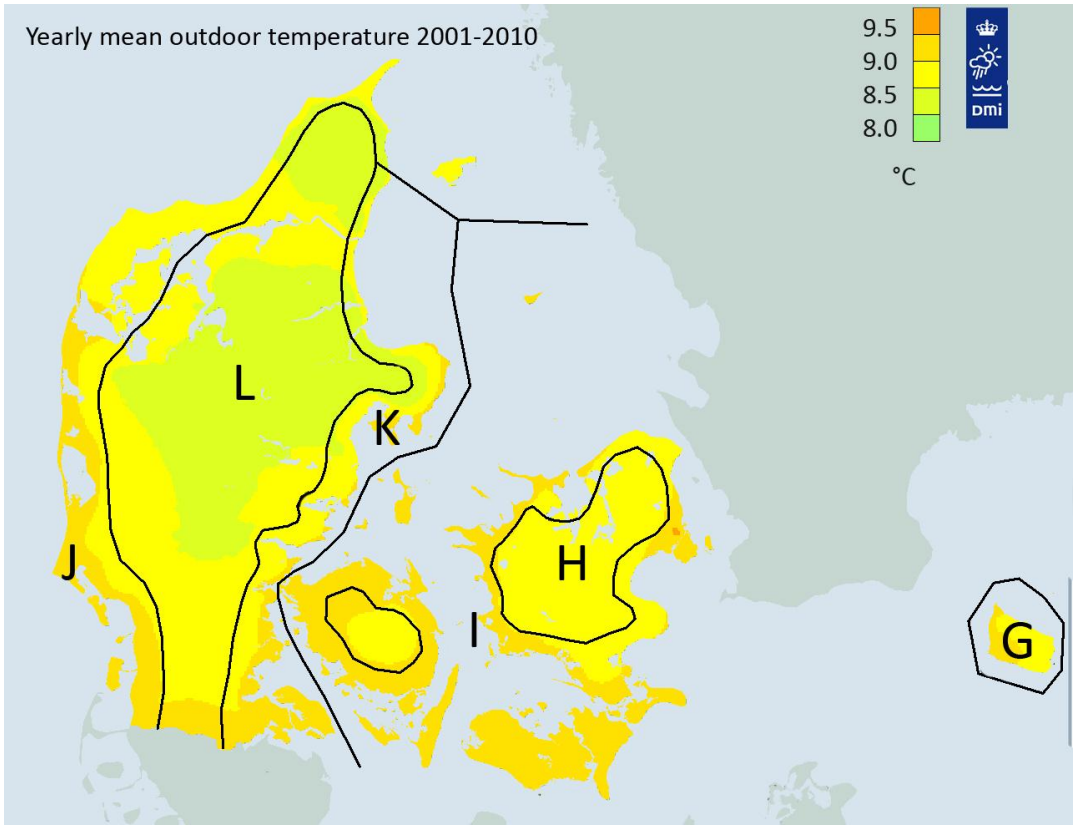

Figure 20 The regions with different outdoor temperatures.

Figure 21 and Figure 22 shows the monthly and yearly global radiation for the old Design Reference Year for Denmark and for the 6 regions with different solar radiation for the new Design Reference Years. It is noticed that the yearly solar radiation in all the new Design Reference Years are higher than the solar radiation in the old Design Reference Year for Denmark. It is also noticed that the solar radiation for Bornholm is very high.

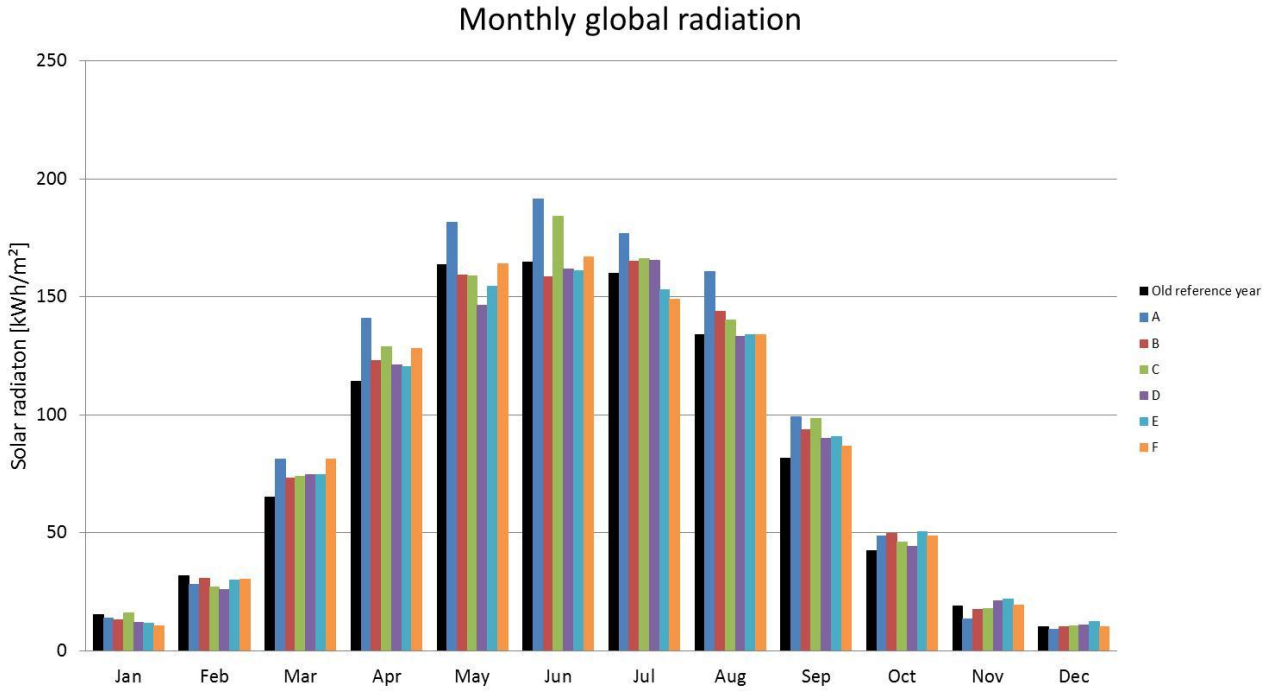

Figure 21 Monthly global radiation for old and new Design Reference Years.

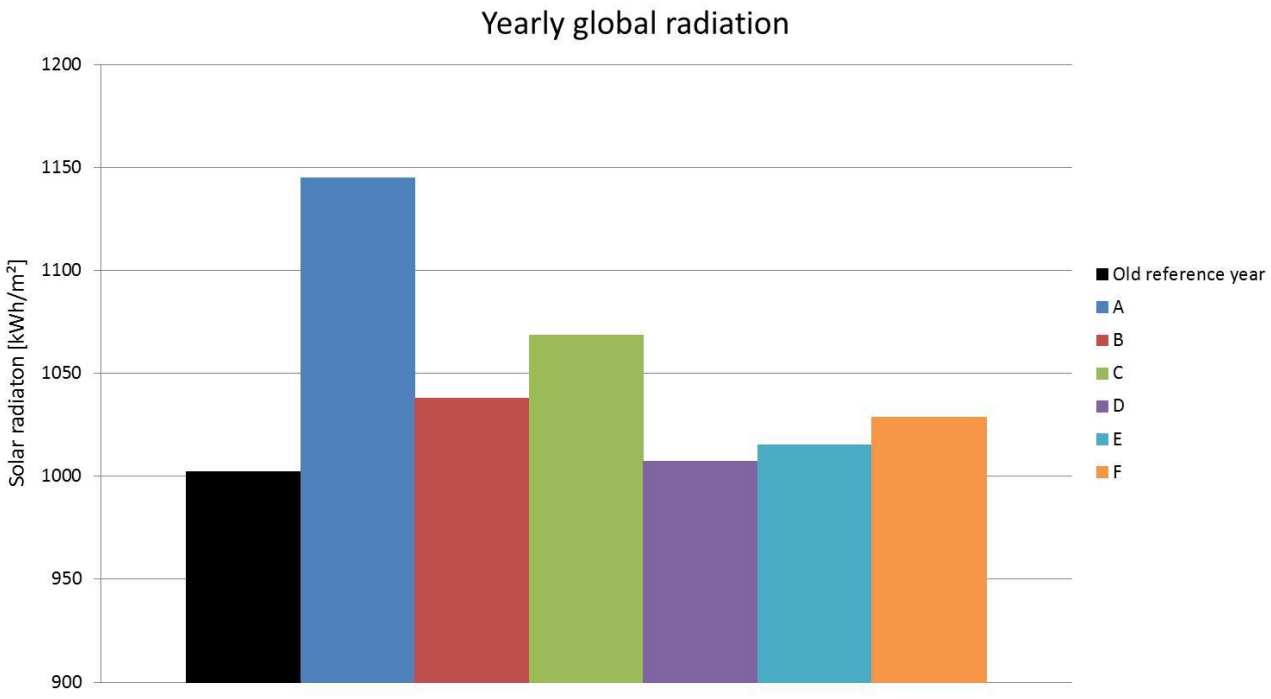

Figure 22 Yearly global radiation for old and new Design Reference Years.

Figure 23 shows the monthly average outdoor temperature for the old Design Reference Year and for the 6 regions with different outdoor temperatures in the new Design Reference Years. The yearly average outdoor temperature in the old Design Reference Year for Denmark is somewhat lower than the yearly average outdoor temperature in the new Design Reference Years .

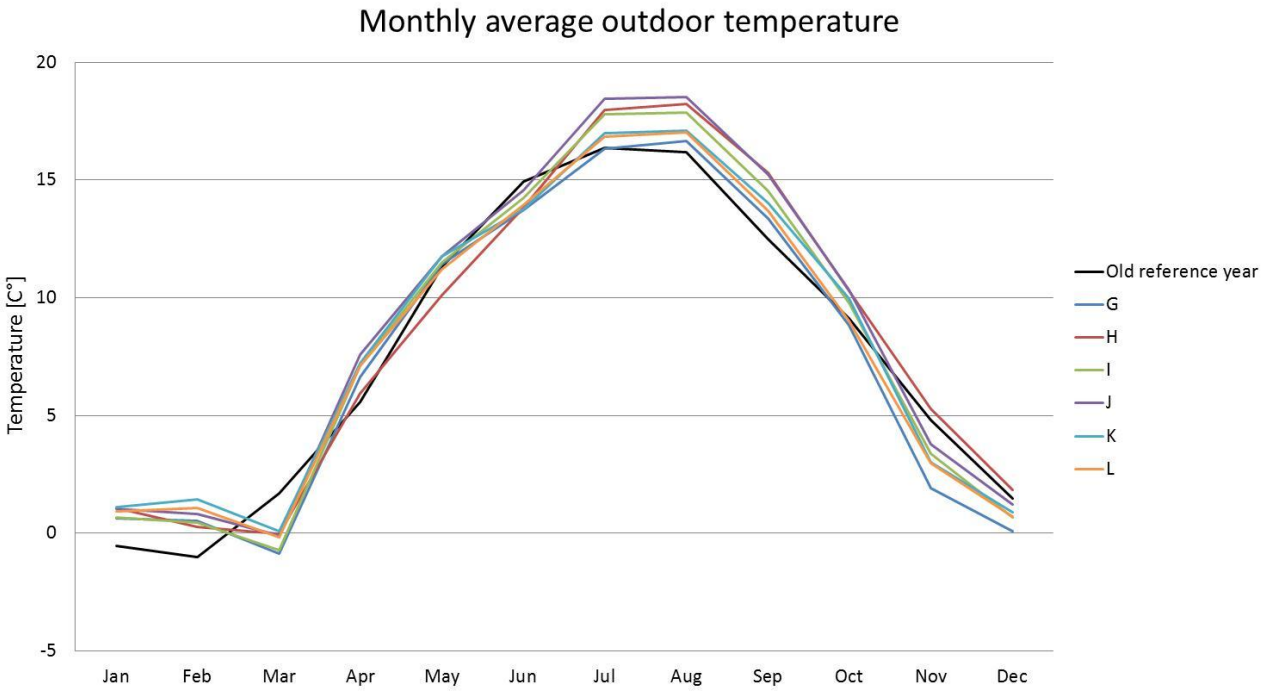

Figure 23 Monthly average outdoor temperatures for old and new Design Reference Years.

Calculations of the yearly thermal performance for two solar collectors for solar heating plants are carried out for the old Design Reference Year for Denmark and for the 19 new Design Reference Years. The thermal performances are calculated for different solar collector fluid temperatures. The solar collector fluid temperature is assumed to be constant during the whole year. The solar collectors are from ARCON Solar, one without an ETFE foil and one with an ETFE foil. The collector efficiencies η are [5]:

Collector without the ETFE foil:

$$\eta = K_\theta \cdot 0.828 - 3.26 \cdot \frac{T_m - T_a}{G} - 0.0086 \cdot \frac{(T_m - T_a)^2}{G}$$

where the incidence angle modifier K_θ is

$$K_\theta = 1 - tan^{3.8}(\theta/2)$$

T_m is the average solar collector fluid temperature, °C

T_a is the ambient temperature, °C

G is the solar irradiance, W/m²

θ is the incidence angle of the beam radiation on the collector, °

Collector with the ETFE foil:

$$\eta = K_\theta \cdot 0.800 - 2.16 \cdot \frac{T_m - T_a}{G} - 0.0119 \cdot \frac{(T_m - T_a)^2}{G}$$

where the incidence angle modifier K_θ is

$$K_\theta = 1 - tan^{3.8}(\theta/2)$$

It is assumed that the collectors are facing south and that the collector tilt is 35° from horizontal. Shadows are disregarded. Figure 24 through Figure 26 show the yearly thermal performance of the collector without the ETFE foil as a function of the mean solar collector fluid temperature for the old Design Reference Year for Denmark and the 19 new Design Reference Years. The extra yearly thermal performances for the new Design Reference Years compared to the old Design Reference Year for Denmark are also shown. The yearly thermal performance for the new Design Reference Year for Bornholm is between 17% and 37% higher than the thermal performance for the old Design Reference Year for Denmark. The extra thermal performance is strongly influenced by the mean solar collector fluid temperature. For increasing mean solar collector temperature the extra percentage thermal performance is increasing. For the other 18 regions the extra thermal performance for the new Design Reference Years compared to the old Design Reference Year for Denmark is in the range from -2% to +31%.

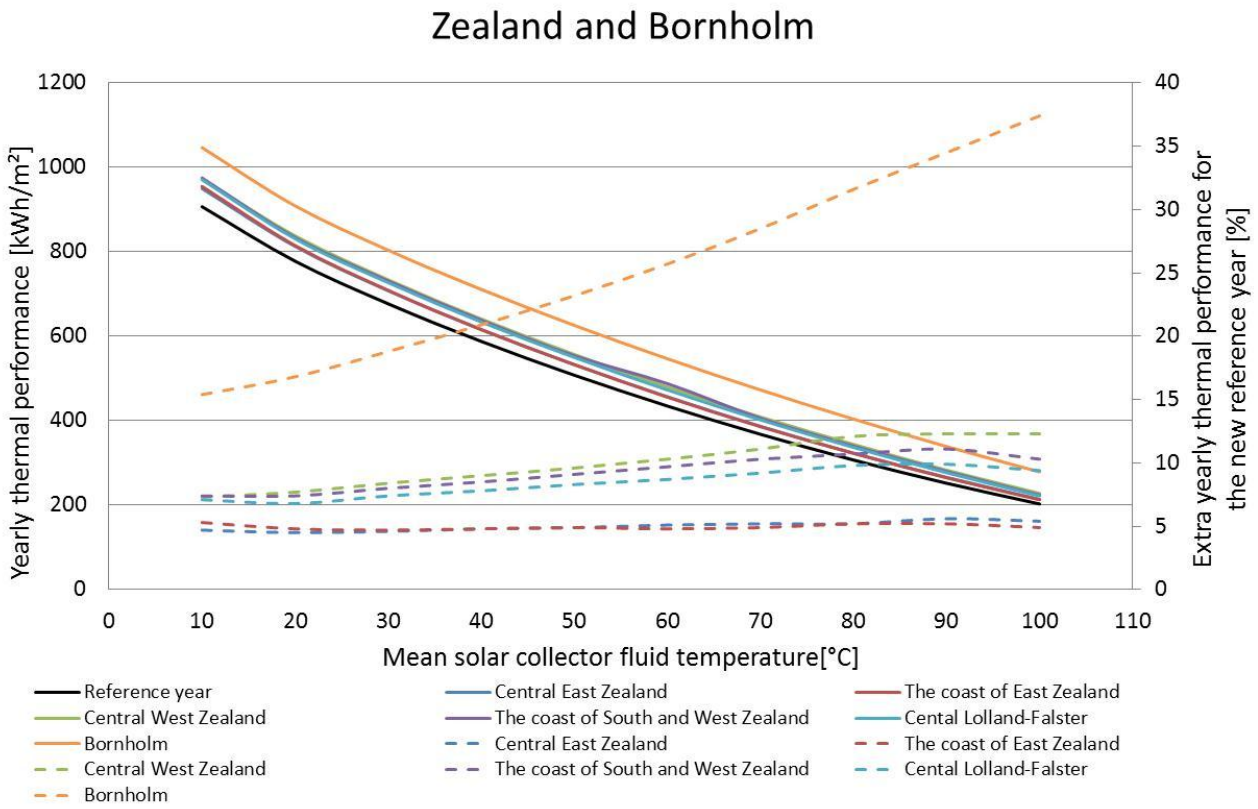

Figure 24 Yearly thermal performance of solar collector without an ETFE foil as function of the mean solar collector fluid temperature for different Design Reference Years for Zealand and Bornholm.

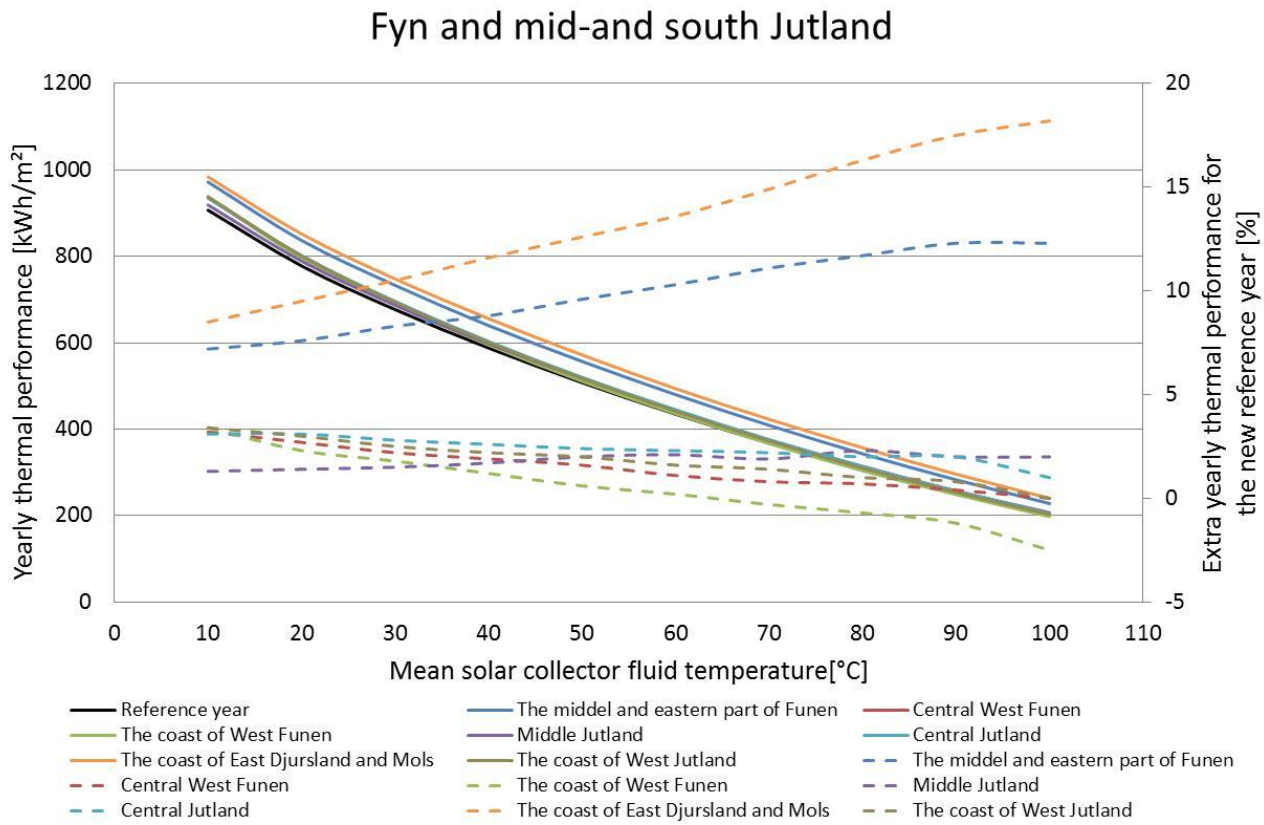

Figure 25 Yearly thermal performance of solar collector without an ETFE foil as function of the mean solar collector fluid temperature for different Design Reference Years for Fyn and mid-and south Jutland

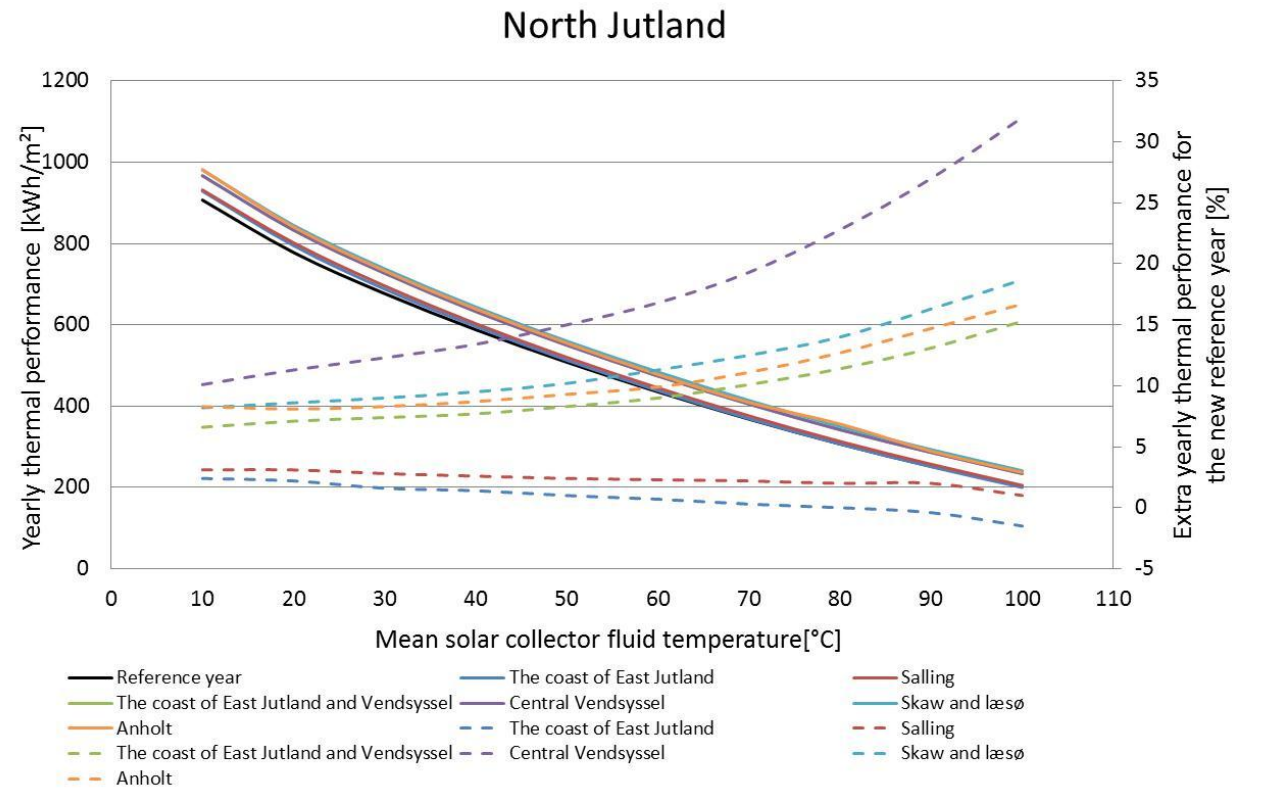

Figure 26 Yearly thermal performance of solar collector without an ETFE foil as function of the mean solar collector fluid temperature for different Design Reference Years for North Jutland.

Figure 27 to Figure 29 shows the yearly thermal performance of the collector with the ETFE foil as a function of the mean solar collector fluid temperature for the old Design Reference Year for Denmark and the 19 new Design Reference Years. The extra yearly thermal performances for the new Design Reference Years compared to the old Design Reference Year for Denmark are also shown. The yearly thermal performance for the new Design Reference Year for Bornholm is between 15% and 34% higher than the thermal performance for the old Design Reference Year for Denmark. The extra thermal performance is strongly influenced by the mean solar collector fluid temperature. For increasing mean solar collector temperature the extra percentage thermal performance is increasing. For the other 18 regions the extra thermal performance for the new Design Reference Years compared to the old Design Reference Year for Denmark is in the range from -2% to +25%.

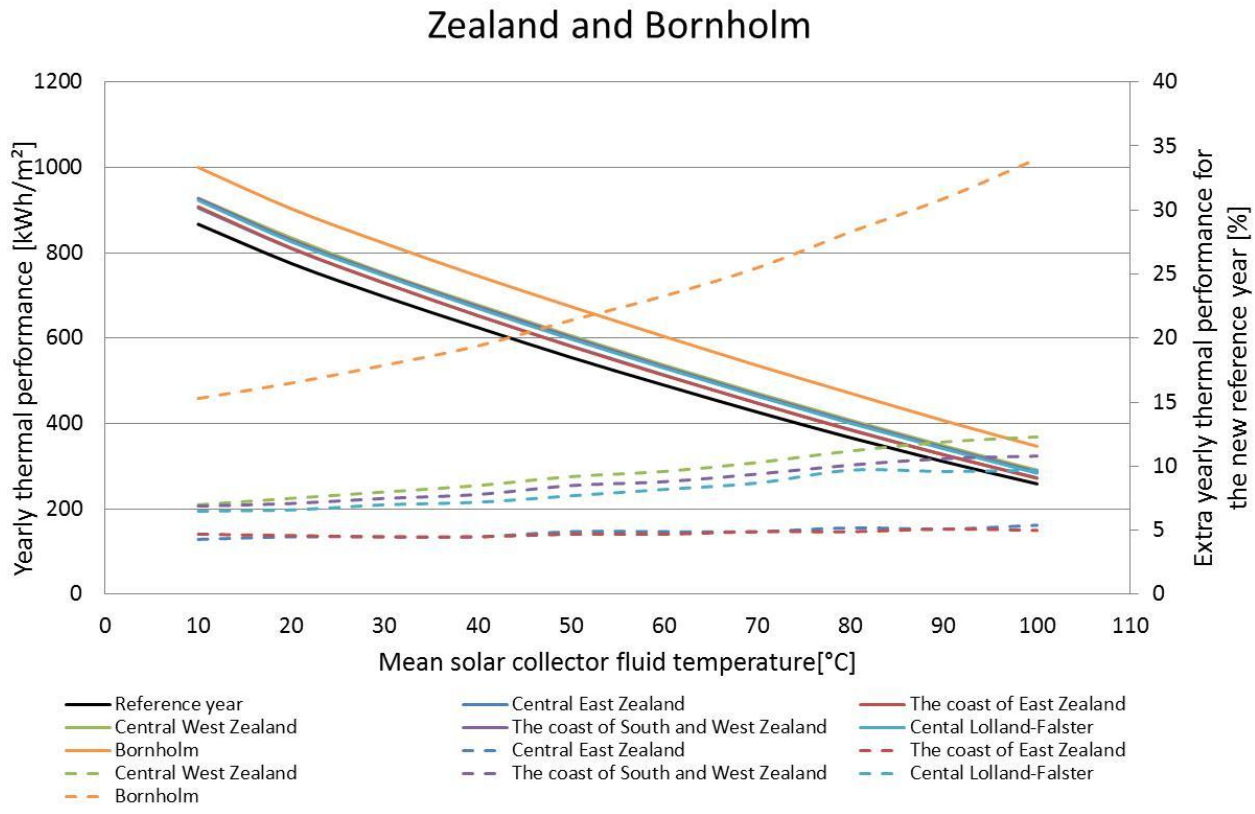

Figure 27 Yearly thermal performance of solar collector with an ETFE foil as function of the mean solar collector fluid temperature for different Design Reference Years for Zealand and Bornholm.

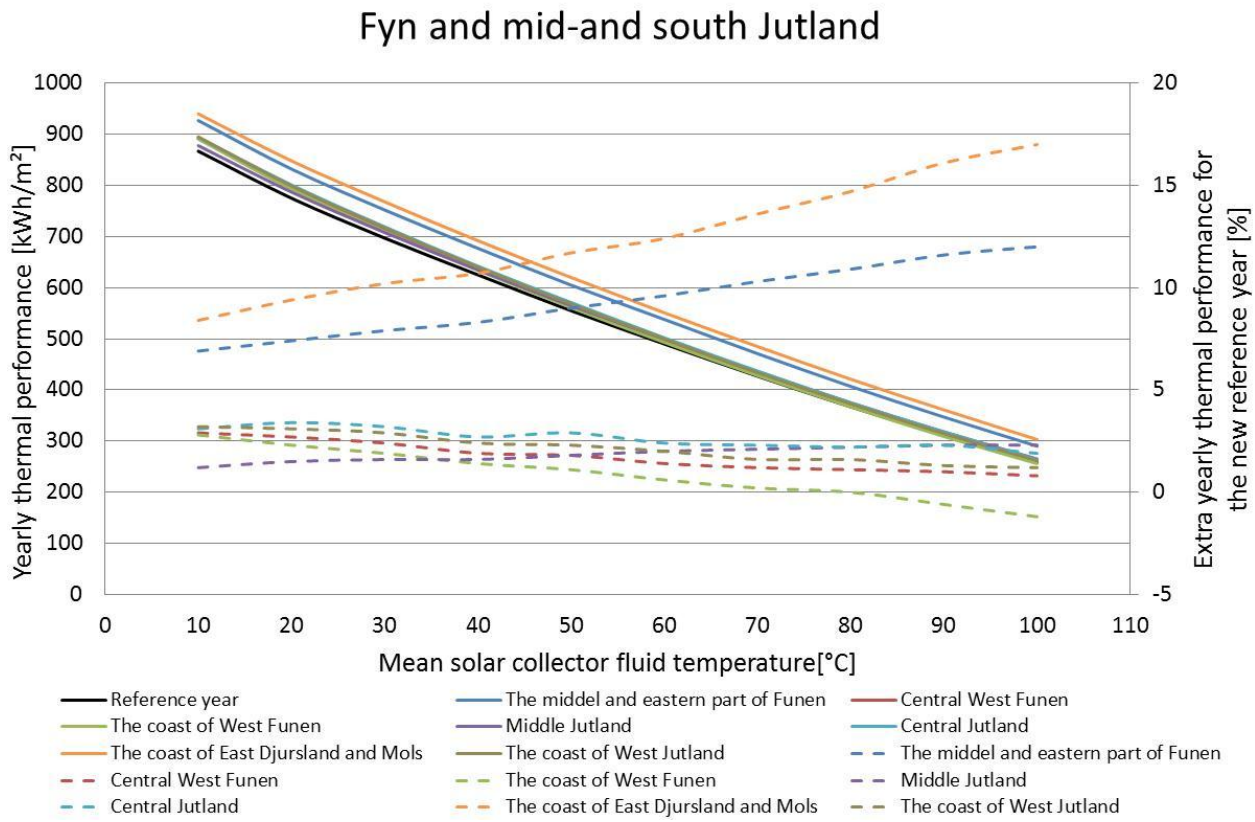

Figure 28 Yearly thermal performance of solar collector with an ETFE foil as function of the mean solar collector fluid temperature for different Design Reference Years for Fyn and mid-and south Jutland

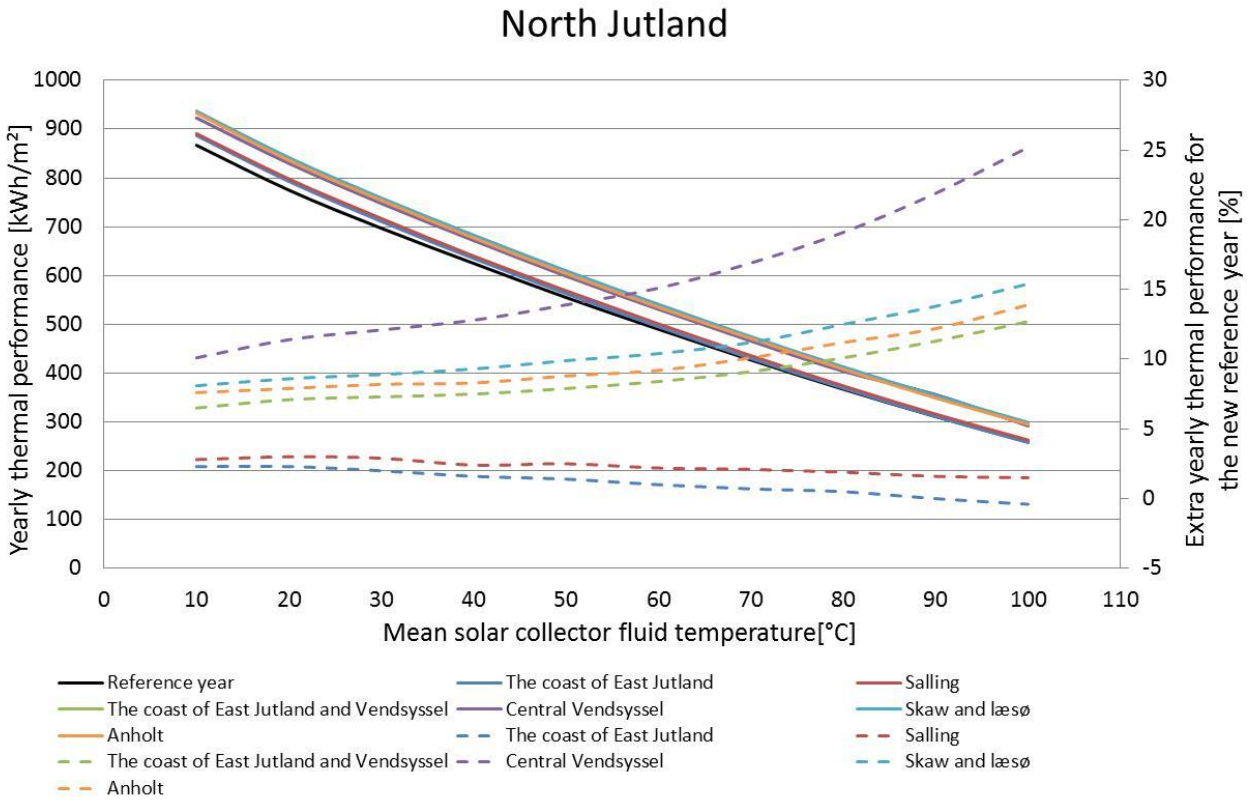

Figure 29 Yearly thermal performance of solar collector with an ETFE foil as function of the mean solar collector fluid temperature for different Design Reference Years for North Jutland

6. Conclusions

Investigations of existing methods to determine diffuse radiation from global radiation measurements showed that the most suitable method is method developed by Skartveit and Olseth. However, it is recommended in the future to develop an improved method.

Calculations of the thermal performance of solar collectors with new Design Reference Years for different regions in Denmark and with the old Design Reference Year for Denmark showed that the thermal performances of solar collectors with the new Design Reference Years are up to 37% higher than the thermal performances of the collectors with the old Design Reference Year for Denmark. There are quite large variations in the thermal performance of solar collectors from region to region. Typical extra thermal performances of solar collectors with the new Design Reference Years compared to thermal performances of collectors with the old Design Reference year are in the range from 2% to 20%.

7. References

[1] Riches, M. R., 1980. “An introduction to meteorological measurements and data handling for solar energy application”. IEA Task IV. U.S. Department of Energy, U.S.A.

[2] Duffie, J. A., Beckman, W. A., 2006. “Solar engineering of thermal processes”, third edition. John Wiley & Sons Inc., U.S.A.

[3] Skarveit, A., Olseth, J. A., Tuft, M. E., 1998. “An hourly diffuse fraction model with correction for variability and surface albedo”. Solar Energy Vol. 63 No. 3, pp. 173-183.

[4] Scharling, M., Riddersholm Wang, P., Pagh Nielsen, K., 2012. “2001-2010 Design Reference Years for Denmark”. Teknisk rapport 12-17, DMI.

[5] Chen, Z., Furbo, S., Perers, B., Fan, J., Andersen, E., 2012. „Efficiencies of flat plate solar collectors at different flow rates”. SHC Conference Proceedings, San Francisco, USA.

DTU Civil Engineering
Department of Civil Engineering
Technical University of Denmark

Brovej, Building 118
2800 Kgs. Lyngby
Telephone 45 25 17 00

www.byg.dtu.dk

ISBN 9788778773593
ISSN 1601-8605